Anti-Müllerian hormone is expressed and secreted by bovine oviductal and endometrial epithelial cells

Raihana Nasrin Ferdousy [1], Onalenna Kereilwe[1], Hiroya Kadokawa[1]*

[1]Joint Faculty of Veterinary Medicine, Yamaguchi University, Yamaguchi-shi, Yamaguchi-ken 1677-1, Japan

Correspondence

Hiroya Kadokawa, Joint Faculty of Veterinary Medicine, Yamaguchi University, Yamaguchi-shi, Yamaguchi-ken 1677-1, Japan.

Email: hiroya@yamaguchi-u.ac.jp

Running head

AMH in bovine oviduct and uterus

Abstract

In this study, we investigated whether bovine oviducts and endometria produce AMH (for paracrine and autocrine signaling). Reverse transcription-polymerase chain reaction and western blotting detected AMH expression in oviductal and endometrial specimens. Immunohistochemistry revealed robust AMH expression in the ampulla and isthmus epithelia, and the glandular and luminal endometrial epithelia (caruncular endometria). *AMH* mRNA (measured by real-time PCR) and protein expression in these layers did not significantly differ among estrous phases in adult Japanese Black (JB) heifers ($P > 0.1$). Furthermore, the expression in these layers also did not differ among Holsteins cows (93.8 ± 5.8 months old), JB heifers (25.5 ± 0.4 months old), and JB cows (97.9 ± 7.9 months old). We also compared AMH concentrations in the oviduct and uterine horn fluids among the three groups (measured by immunoassays). Interestingly, the AMH concentration in the oviduct fluid, but not in the uterine horn fluid, of Holsteins cows, were lower than those in JB heifers and cows ($P < 0.05$). Therefore, bovine oviducts and endometria express AMH and likely secrete it into the oviduct and uterine fluids.

KEY WORDS

age, AMH receptor type 2, Holstein dairy cow, Müllerian-inhibiting substance, ruminant

1 INTRODUCTION

Anti-Müllerian hormone (AMH) is a member of the transforming growth factor (TGF)-β family. Preantral and small antral follicles secrete AMH in female animals (Bhide & Homburg, 2016). AMH expression is well-characterized in ovaries and plays important roles in regulating follicular development (Hernandez-Medrano et al., 2012) and inhibiting follicular atresia (Sefrioui et al., 2019). Concentrations of circulating AMH can help to predict the number of high-quality embryos produced by various mammals, including cows and humans (Arouche et al., 2015; Sefrioui et al., 2019). High-quality embryos result from synchronous regulation by the sperm, ovum, oviduct, and endometrium. Further, plasma AMH concentrations are positively correlated with pregnancy rates in various animals, including humans and cows (Ribeiro et al., 2014; Josso, 2019).

Accordingly, women with low blood AMH concentrations have an increased risk of miscarriage (Tarasconi et al., 2017; Lyttle et al., 2018). Moreover, mares with delayed uterine clearance have significantly lower blood AMH concentrations than those without delayed uterine clearance (Gharagozlou et al., 2013). Therefore, AMH might play vital roles in the oviduct and endometrium. Anti-Müllerian hormone can act at the extragonadal level by activating its primary receptor, AMH receptor type 2 (AMHR2), in the gonadotrophs of anterior pituitaries of rats and bovines (Garrel et al., 2016; Kereilwe & Kadokawa, 2019). We have previously shown that bovine gonadotrophs express AMH, which likely acts in paracrine and autocrine manner (Kereilwe et al., 2018). Endometrial tissues of healthy women also express AMHR2 (Kim et al., 2019). We recently discovered that AMHR2 is expressed in parts of the bovine oviducts and uterus that are important for fertility and

embryogenesis, namely, the epithelium of the tunica mucosa of the ampulla and isthmus, the epithelium of uterine glands, and the luminal epithelium of the endometrium (Ferdousy et al., 2020). Therefore, these tissues might express AMH for different paracrine and autocrine roles.

Old age is associated with decreased fertility in cows and humans (Osoro & Wright, 1992; Scheffer et al., 2018); however, the exact mechanisms underlying this association remains unclear. Several studies in humans have linked aging to plasma AMH concentrations. Blood AMH concentrations are highest in pubertal girls and gradually decrease starting at age 25 until they are undetectable after menopause (Dewailly et al., 2014), suggesting that low AMH is a marker of ovarian aging (Bhide & Homburg, 2016). Studies on the relationship between age and plasma AMH concentrations in adult female ruminants are not common, but one study showed that Japanese Black cows have higher blood AMH concentrations than post-pubertal heifers (Koizumi & Kadokawa, 2017). Therefore, age might be a determinant of AMH expression levels in the oviducts and endometria, although there could be species-specific differences as well.

Therefore, in this study, we evaluated the association between oviductal and endometrial AMH expression and various physiological factors, such as the stage of the estrous cycle, age, and breed. We also compared AMH concentrations in the oviduct and uterine horn fluids collected from Holsteins cows and Japanese Black heifers and cows.

2 MATERIALS AND METHODS

All experiments were performed according to the Guiding Principles for the Care and Use of Experimental Animals in the Field of Physiological Sciences (Physiological Society of Japan) and approved by the Committee on Animal Experiments of Yamaguchi University (approval no. 301).

2.1 Sample collection

We obtained oviductal and endometrial samples from cattle managed by contract farmers in western Japan. All cattle born in Japan since 2003 are registered at birth with an individual identification number in a database of National Livestock Breeding Center of Japan. We utilized both individual identification numbers to search the database and information given by the contract farmers for the cattle in this study.

2.2 Experiment 1

Experiment 1 was conducted to evaluate whether AMH was expressed in the oviduct and endometrium in heifers utilizing reverse transcription-polymerase chain reaction (RT-PCR), western blotting, and immunofluorescence staining. We obtained the ipsilateral side of the ampulla, isthmus, caruncular, and intercaruncular area of endometria from four post-pubertal (26 months of age) Japanese Black heifers at a local abattoir. The four heifers were at days 2 to 3, 8 to 12, 15 to 17, and 19 to 21 (day 0 = day of estrus), as determined via macroscopic examination of the ovaries and uterus (Miyamoto et al., 2000). The ampulla, isthmus, caruncle, and intercaruncle samples collected were from the side ipsilateral to ovulation in the three heifers from days 2 to 3, 8 to 12, or 15 to 17 but were from the side ipsilateral to the dominant follicle in the remaining heifer at day 19 to 21. We collected

ampullar samples from areas at least 3 cm from the fimbriated infundibulum, from the ampullary–isthmic junction, and the isthmus samples from areas also at least 3 cm from the ampullary–isthmic junction, and the utero-tubal junction. Half of the ampulla and half of the isthmus were frozen in liquid nitrogen and preserved at −80 °C until RNA or protein extraction. The remaining halves of the ampulla and isthmus were stored in 4% paraformaldehyde at 4 °C for 16 hr for immunohistochemistry. The middle area of the uterine horn was opened longitudinally using scissors, and caruncle tissues were carefully dissected so as not to include the intercaruncle; then, intercaruncle areas were excised. The collected caruncle and intercaruncle samples were frozen in liquid nitrogen and preserved at −80 °C until RNA or protein extraction or stored in 4% paraformaldehyde at 4 °C for 16 hr for immunohistochemistry. Granulosa cells in preantral and small antral follicles express AMH (Campbell et al., 2012; Kereilwe et al., 2018). Therefore, we also collected ovarian tissue samples from the same heifers to use as a positive control of AMH expression for RT-PCR and western blotting assays.

2.3 Experiment 2

Experiment 2 was conducted to compare AMH expression in oviductal and endometrial samples among different stages of the estrous cycle utilizing quantitative RT-PCR and western blotting described subsequently. The ampulla, isthmus, caruncle, and intercaruncle tissues were harvested from adult (26-month-old) non-pregnant Japanese Black heifers in the pre-ovulatory phase (day 19 to 21; n = 5), day 1 to 3 (n = 5), day 8 to 12 (n = 5), or day 15 to 17 (n = 5), as determined via macroscopic examination of the ovaries and

uterus (Miyamoto et al., 2000). Samples were obtained at the local abattoir and immediately frozen in liquid nitrogen and preserved at −80 °C until RNA or protein extraction.

2.4 Experiment 3

Experiment 3 was conducted to compare AMH expression in oviductal and endometrial samples based on age or breed utilizing the quantitative RT-PCR and western blotting described subsequently. The ampulla, isthmus, caruncle, and intercaruncle tissues were harvested during the luteal phase (day 8 to 12) from post-pubertal Japanese Blacks heifers (25.5 ± 0.4 months of age; n = 6), Japanese Black cows (97.9 ± 7.9 months of age; n = 6), and Holstein cows (93.8 ± 5.8 months of age; n = 6) from the local abattoir. We compared these three groups due to the following reasons. First, it was impossible to obtain samples from post-pubertal Holstein heifers since they were kept in dairy farms for milking purposes. Second, in our previous study (Kereilwe et al., 2018), we compared expression levels of AMH in gonadotrophs between Holsteins cows (approximately 80 months of age), and Japanese Black heifers (approximately 26 months of age) and cows (approximately 90 months of age), finding significant differences in *AMH* mRNA and AMH protein among them. Third, we previously observed a significant difference in blood AMH concentrations between Japanese Black cows (approximately 81 months of age) and Japanese Black heifers (approximately 22 months of age) (Koizumi & Kadokawa, 2017). The collected samples were frozen in liquid nitrogen and preserved at −80 °C until RNA or protein extraction. All heifers and cows in the three groups were non-lactating and non-pregnant, with no follicular cysts, luteal cysts, or other ovarian or uterine disorders upon macroscopic ovarian

examination (Kamomae, 2012). The Holstein cows were slaughtered because they had not become pregnant after at least five artificial insemination attempts.

2.5 Experiment 4

Experiment 4 was conducted to analyze AMH concentrations in the oviduct and uterine horn fluids using an AMH enzyme immunoassay. We collected oviduct fluids on day 1 to 3, i.e. when oocytes are in oviduct (El-Banna & Hafez, 1970), and uterine horn fluids on day 8 to 14 in order to compare AMH concentrations among groups of Japanese Black heifers (26.2 ± 0.7 months of age; n = 6), Japanese Black cows (111.0 ± 12.2 months of age; n = 6), and Holstein cows (91.9 ± 6.4 months of age; n = 6). The females were killed at the slaughterhouse; the ipsilateral sides of oviducts to ovulation were closed at the uterine end and then cut to separate the uterine end from the utero-tubal junction. The oviducts were then separated from the surrounding connective tissue. A blunt 20-gauge needle was inserted from the infundibulum side of the oviducts and used to gently flush the oviducts with 0.01 M phosphate-buffered 0.14 M saline (pH 7.3) (PBS; 2 mL/oviduct). The resultant oviductal fluids were collected from the opposite sides of the oviducts and pooled into 2-mL microtubes. For the collection of uterine fluids, a blunt 20-gauge needle was inserted into the tip of a cut uterine horn in which the uterine-body side had been closed by artery forceps. After gently flushing with PBS (10 mL/horn), the resultant fluids were collected from the tip of the cut uterine horn and pooled into 50-mL tubes. Tubes were centrifuged at 800 × g for 20 min at 4° C, and the supernatants were stored at –35° C until analyzed for AMH.

2.6 RT-PCR, sequencing of amplified products, and homology search in gene databases

We utilized the same RT-PCR and sequencing methods as reported previously (Kereilwe et al., 2018) to determine the expression of AMH mRNA in the ovary, ampulla, isthmus, caruncle, or intercaruncle from the four heifers for experiment 1. Briefly, total RNA was extracted from the samples using RNAzol RT Reagent (Molecular Research Center Inc., Cincinnati, OH, USA) according to the manufacturer's protocol. The extracted RNA samples were treated with ribonuclease-free deoxyribonuclease (Thermo Fisher Scientific, Waltham, MA, USA) to eliminate possible genomic DNA contamination. The concentration and purity of each RNA sample were evaluated to ensure that the A260/A280 nm ratios were in the acceptable range of 1.8–2.1. The mRNA quality of all samples was verified by electrophoresis of total RNA followed by staining with ethidium bromide, and confirming that the 28S:18S ratios were 2:1. The cDNA was synthesized from 1 µg of the total RNA per sample using SuperScript IV VILO Master Mix (Thermo Fisher Scientific) according to the manufacturer's protocol. No reverse transcription controls (NRCs) were prepared for RT-PCR; they were generated by treating the extracted RNA with the same deoxyribonuclease but not with cDNA synthetase. PCR was conducted using the previously reported primers (Kereilwe et al., 2018): nucleotides 1486–1813, forward primer: 5′-GCTCATCCCCGAGACATACC-3′; reverse primer: 5′-TTCCCGTGTTTAATGGGGCA-3′). Primers were designed by the Primer3 algorithm (https://www.ncbi.nlm.nih.gov/tools/primer-blast/) based on a reference sequence of bovine AMH [the National Center for Biotechnology Information (NCBI) reference sequence of bovine AMH is NM_173890]. The expected PCR-product size of AMH using the primer pair is 328 bp. Using a Veriti 96-Well Thermal Cycler (Thermo Fisher Scientific), PCR was

performed using 20 ng of cDNA, 20 ng RNA as the NRC or water as the no template control (NTC), and polymerase (Tks Gflex DNA Polymerase, Takara Bio Inc., Shiga, Japan) under the following thermocycling conditions: 94 °C for 1 min for pre-denaturation followed by 35 cycles of 94 °C for 60 sec, 60 °C for 15 sec, and 68 °C for 30 sec. PCR products were separated on 1.5% agarose gels by electrophoresis along with a molecular marker [Gene Ladder 100 (0.1–2 kbp), Nippon Gene, Tokyo, Japan], stained with fluorescent stain (Gelstar, Lonza, Allendale, NJ, USA), and observed using a charge-coupled device (CCD) imaging system (GelDoc; Bio-Rad, Hercules, CA, USA). The PCR products were purified with the NucleoSpin Extract II kit (Takara Bio Inc.) and subsequently, sequenced with a sequencer (ABI3130, Thermo Fisher Scientific) using one of the PCR primers and the Dye Terminator v3.1 Cycle Sequencing Kit (Thermo Fisher Scientific). The sequences obtained were used as query terms to search the homology sequence in the DNA Data Bank of NCBI using the basic nucleotide local alignment search tool (BLAST) optimized for highly similar sequences (available on the NCBI website).

2.7 Anti-AMH antibody used in this study

We utilized the same anti-human AMH rabbit polyclonal antibody (ARP54312; Aviva Systems Biology, CA, USA) that we previously verified with bovine ovaries (Kereilwe et al., 2018) to determine the expression of AMH in the bovine samples by western blotting and immunohistochemistry. Human AMH is secreted as a homodimeric precursor consisting of two identical monomers (560 amino acids; NCBI accession number AAA98805.1) (Mamsen et al., 2015). Each monomer consists of two domains, specifically (i) a mature C-terminal region, which becomes bioactive after proteolytic cleavage and binds

AMHR2, and (ii) a pro-region, which is important for AMH synthesis and extracellular transport. The human AMH precursor is cleaved at amino acid 451 (arginine) between the two domains. The pro-region has another cleavage site at amino acid 229 (arginine), causing three potential cleavage products, namely pro-mid-mature, mid-mature, and mature (Mamsen et al., 2015). The bovine AMH precursor monomer (575 amino acids; NCBI accession number NP_776315.1) has a 91% sequence homology to the human protein. The bovine AMH precursor contains an arginine cleavage site between the two domains at amino acid 466 but not at the residue corresponding to amino acid 229. The rabbit polyclonal anti-AMH antibody recognizes the mature C-terminal form of human AMH (corresponding to amino acids 468–517; SVDLRAERSVLIPETYQANNCQGVCGWPQSDRNPRYGNHVVLLLKMQARG). This sequence has 98% homology to amino acids 483–532 of the mature C-terminal form of bovine AMH but no homology to other bovine proteins, as determined based on protein BLAST.

2.8 Western blotting for AMH detection

Western blotting was performed as described previously (Kereilwe et al., 2018). Briefly, proteins were extracted from the ampulla, isthmus, caruncle, intercaruncle, or ovary samples (used as positive controls) from the four heifers used in experiment 1. The extracted protein sample (33.4 µg of total protein in 37.5 µl) was mixed in 12.5 µl of 4× Laemmli sample buffer (Bio-rad) containing 10% (v/v) β-mercaptoethanol, and then boiled for 3 min at 100 °C. The boiled protein samples were quickly cooled on ice. Then, 12 µl of boiled protein samples

(8 μg of total protein) was loaded onto a sodium dodecyl sulfate-polyacrylamide polyacrylamide gel (Any KD Criterion TGX precast gel; 567-1125; Bio-Rad) along with a molecular weight marker (Precision Plus Protein All Blue Standards; Bio-Rad) and resolved by electrophoresis at 100 V for 90 min. Proteins were then transferred to polyvinylidene fluoride (PVDF) membranes. Blocking was performed with 5% non-fat dry milk containing 0.1% tween 20 for 1 hr at 25 °C; subsequently, immunoblotting was performed with the anti-AMH rabbit antibody (1:25,000 dilution) overnight at 4 °C. After washing the membrane with 10 mM tris–HCl (pH 7.6) containing 150 mM NaCl and 0.1% tween 20, the PVDF membrane was incubated with horseradish peroxidase (HRP)-conjugated anti-rabbit IgG goat antibody (Bethyl Laboratories, Inc., Montgomery, TX, US; 1:50,000 dilution) for 1 hr at 25 °C. Protein bands were visualized using an ECL-Prime chemiluminescence kit (GE Healthcare, Amersham, UK) and CCD imaging system (Fujifilm, Tokyo, Japan). We defined bovine AMH bands based on band size as the AMH precursor or the mature form (four sizes) according to previous studies (Mamsen et al., 2015; Kereilwe et al., 2018). Antibodies were removed from the PVDF membrane with a stripping solution (Nacalai Tesque Inc., Kyoto, Japan); then, the membrane was used for immunoblotting with the anti-β-actin mouse monoclonal antibody (A2228, 1:50,000 dilution; Sigma-Aldrich, St. Louis, MO, USA).

Western blotting was also conducted to compare AMH protein expression levels in the ampulla, isthmus, caruncle, and intercaruncle among different estrous phases or the groups of Japanese Black heifers, Japanese Black cows, and Holstein cows from experiment 2 or 3. Briefly, boiled samples (8 μg total protein of each sample) were loaded on a polyacrylamide gel along with the molecular weight marker and four standard samples (2, 4, 8, and 16 μg

total protein for each of five randomly selected samples diluted with protein extraction reagent). MultiGauge v.3.0 software (Fujifilm) was used to quantify the signal intensity of the protein bands. The intensities of bands representing AMH (as the mature C-terminal form) for 16, 8, 4, and 2 μg protein samples were set as 100%, 50%, 25%, and 12.5%, respectively, and the intensity of other samples was calculated as a percentage of these standards using MultiGauge software. After antibodies were removed from the PVDF membrane with a stripping solution, the membrane was used for immunoblotting with the anti-β-actin mouse monoclonal antibody. The intensities of the β-actin band for 16, 8, 4, and 2 μg protein samples were set as 100%, 50%, 25%, and 12.5%, respectively, and the intensity of other samples was calculated as a percentage of these standards using MultiGauge software. The AMH expression level was normalized to that of β-actin in each sample.

2.9 Fluorescent immunohistochemistry and confocal microscopy

We utilized the same method of immunohistochemistry to detect ovarian AMH and AMHR2 as reported previously (Kereilwe et al., 2018; Kereilwe & Kadokawa, 2019) for experiment 1. Briefly, the fixed tissue blocks were placed in 30% sucrose PBS until the blocks were infiltrated with sucrose. The blocks were then frozen in an embedding medium (Tissue-Tek OCT compound; Sakura Finetechnical Co. Ltd, Tokyo, Japan) and maintained at –80°C. Next, the blocks were sectioned into 15-μm-thick cross-sections using a cryostat (Leica Microsystems Pty Ltd, Wetzlar, Germany) and mounted on microscope slides (MAS coat Superfrost; Matsunami-Glass, Osaka, Japan). The sections were treated with 0.3 %

282 triton X-100-PBS for 15 min and blocked by incubating them with 0.5 mL of PBS containing
283 10% normal goat serum (Wako Pure Chemicals, Osaka, Japan) for 1 hr at room temperature.
284 The slides were incubated with a cocktail of primary antibodies containing the anti-AMH
285 (Kereilwe et al., 2018), anti-AMHR2 (Kereilwe & Kadokawa, 2019), anti-cytokeratin
286 antibodies (Sigma-Aldrich) (all diluted as 1:1,000) for 12 hr at 4 °C. After the primary
287 antibody incubation, the sections were washed twice with PBS and then incubated with a
288 cocktail of fluorochrome-conjugated secondary antibodies (Alexa Fluor 488 goat anti-
289 chicken IgG, Alexa Fluor 546 goat anti-mouse IgG, and Alexa Fluor 647 goat anti-rabbit IgG
290 [all from Thermo Fisher Scientific and diluted to 1 μg/mL]) and 1 μg/mL of 4′, 6′-diamino-
291 2-phenylindole (DAPI; Wako Pure Chemicals, Osaka, Japan) for 4 hr at room temperature.
292 The stained sections on slides were observed by confocal microscopy (LSM710; Carl
293 Zeiss, Göttingen, Germany) equipped with a diode laser 405 nm, argon laser 488 nm, and
294 HeNe laser 533 nm. Images obtained by fluorescence microscopy were scanned with a 20×,
295 40×, 63× or 100× objective and recorded with a CCD camera system controlled by ZEN2012
296 black edition software (Carl Zeiss). The DAPI is shown in blue, and AMH is shown in green
297 in the confocal images. To verify the specificity of the signals, we included several negative
298 controls in which the primary antiserum had been omitted, or in which normal rabbit IgG,
299 normal mouse IgG, and normal chicken IgG (all from Wako Pure Chemicals) were used
300 instead of the primary antibody.
301

302 **2.10 Quantitative RT-PCR**

Quantitative RT-PCR was performed to compare *AMH* expression among estrous phases or the groups of Japanese Black heifers, Japanese Black cows, and Holstein cows in experiment 2 or 3. The preparation of high-quality total RNA and cDNA synthesis were performed as described herein. We utilized the same method of quantitative RT-PCR and the same primers to measure *AMH* mRNA or two housekeeping genes, *C2orf29* (NCBI accession number XM_002691150.2) and *SUZ12* (NCBI accession number NM_001205587.1), as reported previously (Nahar & Kadokawa 2017; Kereilwe et al., 2018). Table 1 lists the primer sequences for *AMH* and the two housekeeping genes. The two housekeeping genes were selected since they are the most stable and reliable housekeeping genes in the bovine oviducts and endometria (Walker et al., 2009; Nahar & Kadokawa 2017) based on both geNorm and Normfinder programs (Vandesompele, 2002; Nahar & Kadokawa 2017).

Levels of gene expression were measured in duplicate by quantitative RT-PCR analyses with 20 ng cDNA, using the CFX96 Real Time PCR System (Bio-Rad) and Power SYBR Green PCR Master Mix (Thermo Fisher Scientific), with a six-point relative standard curve, the NTC, and the NRC. Standard 10-fold dilutions of purified and amplified cDNA fragments were prepared. The cycle conditions for all genes were: 95 °C for 10 min for pre-denaturation; five cycles each of 95 °C for 15 sec and 66 °C for 30 sec; 40 cycles each of 95 °C for 15 sec, and 60 °C for 60 sec. Melting curve analyses were performed at 95 °C for each amplicon and each annealing temperature to ensure the absence of smaller non-specific products, such as dimers. To optimize the quantitative RT-PCR assay, serial dilutions of a cDNA template were used to generate a standard curve by plotting the log of the starting quantity of the dilution factor against the C_q value obtained during amplification of each

dilution. Reactions with a coefficient of determination (R^2) > 0.98 and efficiency between 95 and 105% were optimized. The coefficients of variation of quantitative RT-PCRs were less than 6%. The concentration of PCR products was calculated by comparing the C_q values of unknown samples with the standard curve using software (CFXmanagerV3.1, Bio-Rad). The gene expression levels of *AMH* genes were normalized to the geometric mean of the expression levels of two housekeeping genes; thus, the *AMH* amount was divided by the geometric mean of *C2orf29* and *SUZ12* in each sample.

2.11 AMH immunoassay

AMH concentrations in samples of the oviduct and uterine fluids were assessed by using a bovine AMH ELISA kit (Ansh Labs, TX, USA) using a protocol described previously (Akbarinejad et al., 2019). The pair of mouse monoclonal antibodies used has epitopes in the N-terminal or C-terminal of the mature C-terminal form of bovine AMH. The ELISA has no cross-reactivity with bovine LH, FSH, inhibins, and activins (personal communication with Dr. Ajay Kumar of Ansh Labs). The detection limit was 0.011 ng/mL, and the intra- and inter-assay coefficient of variation were 4.3% and 8.6%, respectively.

2.12 Statistical analysis

The statistical analyses were performed using StatView version 5.0 for Windows (SAS Institute, Inc., Cary, NC, USA). The Grubb's test was used to verify the absence of

outliers. The Shapiro-Wilk test or the Lilliefors test were used to evaluate the normality or log-normality of each variable, respectively—all variables were normally distributed. The F-test was used to verify the homogeneity of variance of all variables between estrous stages and ages. Using Grubb's test, we verified that there were no outliers for the variables. Analysis of variance (ANOVA) and Fisher's protected least significant difference (PLSD) test were used to evaluate differences in *AMH* mRNA or protein expression in either the ampulla, isthmus, caruncle, or intercaruncle collected from bovines at different estrous stages or different groups. ANOVA and Fisher's PLSD tests were also used to evaluate differences in the logarithm of AMH concentrations in the oviduct or uterine fluids collected from females at different estrous stages or different groups. The level of significance was set at $P < 0.05$. Data are expressed as mean ± standard error of the mean (SEM).

3 RESULTS

3.1 Experiment 1

An amplicon of 328 bp, indicating AMH, was obtained from samples of the ovary, ampulla, isthmus, caruncle, and intercaruncle and confirmed using agarose gel electrophoresis (Fig. 1). Neither the NTC nor NRC yielded any PCR-amplified products. A homology search against the gene databases for the sequenced amplified products revealed bovine AMH (NM_173890.1) as the best match, with a query coverage of 100%, e-value of 0.0, and maximum alignment identity of 99%. No other bovine gene displayed homology with the PCR-product described, indicating that the amplified product was bovine AMH.

AMH expression in the ampulla, isthmus, caruncle, and intercaruncle, and in ovarian specimens used as positive controls was analyzed via western blotting (Fig. 2). Similar

protein bands for AMH were observed among all the tissue samples (Fig. 2A). The ovary, isthmus, caruncle, and intercaruncle, however, showed multiple bands for full-length AMH, whereas the ampulla showed a single band for full-length AMH. The mature C-terminal form was found only in the ovary and intercaruncle but not in the ampulla, isthmus, and caruncle. No protein bands were observed on the blotting membranes used as negative controls, on which the primary antiserum had been pre-absorbed with an antigen peptide. β-actin was the loading control, as shown in Figure 2b.

Fig. 3 and Fig. 4 show the results of immunofluorescence staining for cytokeratin, AMHR2, and AMH in the ampulla or isthmus samples. Immunohistochemistry revealed robust AMH expression in the epithelium of the tunica mucosa, shown as a cytokeratin-positive layer, of the ampulla (Fig. 3A, 3C) and isthmus (Fig. 4A, 4C), where AMH receptor type 2 was also expressed. Further, fibroblasts, which were cytokeratin-negative, too expressed AMH. Fig. 5 and Fig. 6 show the results of immunofluorescence staining for cytokeratin, AMHR2, and AMH in the caruncle or intercaruncle samples. The strong AMH signals were localized to the luminal epithelium (Fig. 5A, 5C), the vasculature in the stroma (Fig. 5A), and the epithelium of endometrial glands (Fig. 6A, 6C). Negative control staining using the normal IgGs showed no immunostaining signal in these layers or cells (Fig. 3B, 4B, 5B, 6B).

Fig. 3 and Fig. 4 show the results of immunofluorescence staining for cytokeratin, AMHR2, and AMH. Immunohistochemistry revealed robust AMH expression in the epithelium of the tunica mucosa, shown as a cytokeratin-positive layer, of the ampulla (Fig. 3A) and isthmus (Fig. 3C), where AMH receptor type 2 was also expressed. Further, fibroblasts, which were cytokeratin-negative, too expressed AMH. The strong AMH signals

were localized to the luminal epithelium (Fig. 4A), the vasculature in the stroma (Fig. 4A), and the epithelium of endometrial glands (Fig. 4C). Negative control staining using the normal IgGs showed no immunostaining signal in these layers or cells (Fig. 3B, 3D, 4B, 4D).

3.2 Experiment 2

Quantitative RT-PCR and western blotting revealed no significant differences in *AMH* mRNA and protein expression among various estrous phases in the ampulla (Fig. 7A, 7E), isthmus (Fig. 7B, 7F), caruncle (Fig. 7C, 7G), and intercaruncle (Fig. 7D, 7H).

3.3 Experiment 3

There were no significant differences in AMH mRNA and protein expression levels in the ampulla (Fig. 8A, 8E), isthmus (Fig. 8B, 8F), caruncle (Fig. 8C, 8G), and intercaruncle (Fig. 8D, 8H) among the Holsteins cows and the Japanese Black heifers and cows.

3.4 Experiment 4

AMH concentrations in the oviduct fluids on day 1 to 3 of Holsteins cows were lower than those in the oviduct fluids of Japanese Black heifers and cows ($P < 0.05$; Fig. 9A). Anti-Müllerian hormone concentrations in uterine horn fluid on day 8 to 14, did not differ among these three groups (Fig. 9B).

4 DISCUSSION

The results revealed robust high-intensity AMH signals in the tunica mucosa of the ampulla and isthmus, and in the glandular and luminal epithelium of endometria, where AMHR2 is constitutively expressed (Ferdousy et al., 2020). Little is known about AMH expression in the oviduct and endometrium in all species. However, a previous study utilizing immunohistochemistry detected AMH expression in the human endometrium (Wang et al., 2009) and human endometrial cancer tissue (Gowkielewicz et al., 2019). Recently, AMHR2 expression was discovered in healthy human endometrial tissues (Kim et al., 2019). We recently discovered that AMHR2 is expressed in the tunica mucosa of the ampulla and isthmus and the glandular and luminal epithelium of bovine endometria (Ferdousy et al., 2020), and this study validates previous findings. These data led to the speculation of potential roles of AMH and AMHR2 in these layers; however, little is known regarding AMH functions in the oviduct and endometrium. The roles of AMH in these layers might depend on the observed constitutive expression, the downstream cytoplasmic pathway of AMHR2, and other tissue-specific TGF -β family members.

Of note, we need to have in mind that the contribution of extragonadal AMH secretion to the blood AMH concentration is unknown. However, no significant difference was observed in the AMH expression levels among the estrous phases in the ampulla, isthmus, caruncle, and intercaruncle tissues. Previous *in vivo* studies have not reported considerable changes in circulating AMH concentrations during the estrous cycle in ruminants (El-Sheikh et al., 2013; Pfeiffer et al., 2014; Koizumi & Kadokawa, 2017). Concurrent with the present findings, the 5′ -flanking region upstream of the bovine AMH gene lacks the consensus response element sequences for estrogen and progesterone (Kereilwe et al., 2018). Therefore,

AMH expression might not change during the estrous cycle in the tunica mucosa of the ampulla and isthmus, and in the glandular and luminal endometrial epithelia. The constitutively expressed AMH in the layers of the oviduct and uterine horns might not play a temporal role, such as that during sperm capacitation and fertilization.

AMH shares an intracellular pathway with another TGF-β family member, bone morphogenetic protein (BMP) (McLennan & Pankhurst 2015). Bovine oviduct epithelial cells express both BMP and BMP receptors, and BMPs might play autocrine roles at the epithelial lining of the oviduct (Valdecantos et al., 2017). Smas and mothers against decapentaplegic (Smads) are the cytoplasmic pathway for BMP receptors in murine oviduct and uterus (Rodriguez et al., 2016). AMH induce Smad1/5/8 phosphorylation via AMHR2 in human granulosa cells (Merhi 2019). AMH signaling regulates expression of BMP receptor type 2, supports Smad signaling, and influences BMP-dependent signaling in non-small cell lung cancer (Beck et al., 2016). Furthermore, uteri from Smad1/5/4-AMHR2-conditional knockout females exhibit multiple defects in the stroma, epithelium, and smooth muscle layers, and fail to assemble a closed uterine lumen upon embryo implantation, with defective uterine decidualization that lead to pregnancy loss at early to mid-gestation (Rodriguez et al., 2016). Mossa & Ireland (2019) suggested that dairy cows with a low antral follicle count (follicles ≥ 3 mm in diameter) have lower blood concentrations of AMH and their endometrium is thinner than those with high antral follicle counts. Therefore, further studies must clarify whether AMH in bovine oviduct and uterus have important autocrine and/or paracrine roles in uterine function.

Our results on the effects of breed and age on such measurements should be interpreted with caution since we could not obtain specimens from Holsteins heifers. However, despite no differences in the AMH expression levels were observed in the ampulla and isthmus among Holsteins cows and the Japanese Black heifers and cows, the AMH concentration in the oviduct fluids of Holsteins cows were lower than those in oviduct fluids from Japanese Black heifers and cows. The comparable results between Japanese Black heifers and cows were unexpected since Japanese Black cows were reported to have higher blood AMH levels than post-pubertal heifers (Koizumi & Kadokawa, 2017). One possible explanation of our results relates to the relevant AMH source. While the AMH in the oviduct fluids may be a direct result of AMH secretion by the oviductal epithelial cells (and not from the blood circulating levels), the blood AMH concentration is not greatly affected by AMH secreted by the oviductal epithelia. However, Japanese Black cattle were fed for meat production, and Holstein cows were infertile. Therefore, since these animals were raised under varied conditions not only different breed and age, it is difficult to interpret the results. Hence, further studies are needed to clarify age- or breed-related differences in the AMH concentration in fluid samples.

Western blotting showed differences in band strength or size between the oviducts and ovaries. The oviduct samples exhibited weaker bands for the mature C-terminal form of AMH than those of the ovary samples, suggesting that the oviducts store less mature C-terminal protein than the ovaries. The oviduct samples also exhibited weaker bands for the AMH precursor than those of the ovary samples. One possible reason for this difference is that the oviducts express lower levels of AMH precursor compared to the ovaries. Another

possible explanation is that the oviducts secret the C-terminal form soon after maturation without storing it subcellularly.

Western blotting showed differences in the number of full-length AMH bands among the ovary, ampulla, isthmus, caruncle, and intercaruncle. Since, different organs show different patterns of AMH O-glycosylation (Meczekalski et al. 2016; Skaar et al., 2011), therefore, differential glycosylation may explain the differences observed in the full-length form in our study.

Collectively, these results show that bovine oviducts and endometria express AMH and likely secrete AMH into the oviduct and uterine fluids. AMH expression might be useful to assess fertility status in bovines. Further studies must examine the roles of AMH in oviducts and the uterus.

In conclusion, these results show that bovine oviducts and endometria express AMH and likely secrete AMH into the oviduct and uterine fluids.

ACKNOWLEDGEMENT

This research was partly supported by a Grant-in-Aid for Scientific Research (JSPS Kakenhi Grant Number 18H02329) from the Japan Society for the Promotion of Science (Tokyo, Japan) to HK. RNF and OK were supported by MEXT (Ministry of Education, Culture, Sports, Science, and Technology) with a scholarship. The authors thank Ms. Laura Akari Obara for helping sample collection.

CONFLICT OF INTERES

The authors declare that they have no competing interests.

ORCID

Raihana Nasrin Ferdousy:0000-0002-0064-1719

Onalenna Kereilwe: 0000-0003-0341-4332

Hiroya Kadokawa: 0000-0002-8454-9601

REFERENCES

Akbarinejad, V., Gharagozlou, F., Vojgani, M., Shourabi, E., & Makiabadi, M. J. M. (2019). Inferior fertility and higher concentrations of anti-Mullerian hormone in dairy cows with longer anogenital distance. *Domestic Animal Endocrinology*, 68, 47-53. https://doi.org/10.1016/j.domaniend.2019.01.011.

Arouche, N., Picard, J. Y., Monniaux, D., Jamin, S. P., Vigier, B., Josso, N., … Taieb, J. (2015). The BOC ELISA, a ruminant-specific AMH immunoassay, improves the determination of plasma AMH concentration and its correlation with embryo production in cattle. *Theriogenology*, 84, 1397-1404. https://doi.org/10.1016/j.theriogenology.2015.07.026.

Beck, T.N., Korobeynikov, V.A., Kudinov, A.E., Georgopoulos, R., Solanki, N.R., Andrews-Hoke, M., … Golemis, E.A. (2016). Anti-müllerian hormone signaling regulates epithelial plasticity and chemoresistance in lung cancer. *Cell Reports*, 16, 657-671. https://doi.org/10.1016/j.celrep.2016.06.043.

Bhide, P., & Homburg, R. (2016). Anti-Müllerian hormone and polycystic ovary syndrome. *Best Practice and Research Clinical Obstetrics and Gynaecology*, 37, 38-45. doi: 10.1016/j.bpobgyn.2016.03.004.

Campbell, B. K., Clinton, M., & Webb, R. (2012). The role of anti-Müllerian hormone (AMH) during follicle development in a monovulatory species (sheep). *Endocrinology*, 153, 4533-4543. https://doi.org/doi: 10.1210/en.2012-1158.

Dewailly, D., Andersen, C. Y., Balen, A., Broekmans, F., Dilaver, N., Fanchin, R.,… Anderson, R. A. (2014). The physiology and clinical utility of anti-Müllerian hormone in

women. *Human Reproduction Update,* 20, 370–385. https://doi.org/10.1093/humupd/dmt062.

El-Banna, A. A., & Hafez, E. S. (1970). Egg transport in beef cattle. *Journal of Animal Science*, 30, 430–432. https://doi.org/10.2527/jas1970.303430x.

El-Sheikh Ali, H., Kitahara, G., Nibe, K., Yamaguchi, R., Horii, Y., Zaabel, S., & Osawa, T. (2013). Plasma anti-Müllerian hormone as a biomarker for bovine granulosa-theca cell tumors: comparison with immunoreactive inhibin and ovarian steroid concentrations. *Theriogenology,* 80, 940-949. https://doi.org/10.1016/j.theriogenology.2013.07.022.

Ferdousy, R. N., Kereilwe, O., & Kadokawa, H. (2020). Anti-Müllerian hormone receptor type 2 (AMHR2) expression in bovine oviducts and endometria: Comparison of AMHR2 mRNA and protein abundance among old Holstein cows and young and old Wagyu females. *Reproduction, Fertility and Development,* 32, 738-747. https://doi.org/10.1071/RD19121

Garrel, G., Racine, C., L'Hôte, D., Denoyelle, C., Guigon, C. J., di Clemente, N., & Cohen-Tannoudji, J. (2016). Anti-Müllerian hormone: a new actor of sexual dimorphism in pituitary gonadotrope activity before puberty. *Scientific Reports,* 6, 23790. https://doi.org/10.1038/srep23790

Gharagozlou, F., Akbarinejad, V., Youssefi, R., & Rezagholizadeh, A. (2013). Low concentration of anti-Müllerian hormone in mares with delayed uterine clearance. *Journal of Equine Veterinary Science,* 34, 575-577. https://doi.org/10.1016/j.jevs.2013.10.176

Gowkielewicz, M., Lipka, A., Piotrowska, A., Szadurska-Noga, M., Nowakowski, J. J., Dzięgiel, P,, … Majewska, M. (2019). Anti-Müllerian hormone expression in endometrial

cancer tissue. *International Journal of Molecular Sciences* 20, E1325. https://doi.org/10.3390/ijms20061325.

Hernandez-Medrano, J. H., Campbell, B. K., & Webb, R. (2012). Nutritional influences on folliculogenesis. *Reproduction in Domestic Animals*, Suppl. 4, 274-282. https://doi.org/10.1111/j.1439-0531.2012.02086.x.

Josso, N. (2019). Anti-Müllerian hormone: a look back and ahead. *Reproduction,* 158, F81-F89. https://doi.org/10.1530/REP-18-0602

Kamomae, H. (2012). Reproductive disturbance. In T. Nakao, T., Tsumagari, S., & Katagiri. S. (Eds.), *Veterinary Theriogenology* (pp. 283-340). Tokyo, Japan: Buneidou Press.

Kereilwe, O., & Kadokawa, H. (2019). Bovine gonadotrophs express anti-Mullerian hormone (AMH): comparison of AMH mRNA and protein expression levels between old Holsteins and young and old Japanese Black females. *Reproduction, Fertility and Development,* 31, 810-819. https://doi.org/10.1071/RD18341.

Kereilwe, O., Pandey, K., Borromeo, V., & Kadokawa, H. (2018). Anti-Müllerian hormone receptor type 2 is expressed in gonadotrophs of postpubertal heifers to control gonadotrophin secretion. *Reproduction, Fertility and Development,* 30, 1192-1203. https://doi.org/10.1071/RD17377.

Kim, S. M., Kim, Y. O., Lee, M. K., Chung, Y. J., Jeung, I. C., Kim, M. R., & Kim, J. H. (2019). Müllerian inhibiting substance/anti-Müllerian hormone type II receptor protein and mRNA expression in the healthy and cancerous endometria. *Oncology Letters*, 17, 532-538. https://doi.org/10.3892/ol.2018.9565.

Koizumi, M., & Kadokawa, H. (2017). Positive correlations of age and parity with plasma

anti-Müllerian hormone concentrations in Japanese Black cows. *Journal of Reproduction and Development*, 63, 205-209. https://doi.org/10.1262/jrd.2016-088.

Lyttle, S. B. M., Jukic, A. M. Z., & Steiner, A. Z. (2018). Antimullerian hormone as a risk factor for miscarriage in naturally conceived pregnancies. *Fertility and Sterility*, 109, 1065-1071. https://doi.org/10.1016/j.fertnstert.2018.01.039.

Mamsen, L. S., Petersen, T. S., Jeppesen, J. V., Møllgard, K., Grøndahl, M. L., Larsen, A., … Andersen, C. Y., (2015). Proteolytic processing of anti-Mullerian hormone differs between human fetal testes and adult ovaries. *Molecular Human Reproduction*, 21, 571–582. https://doi.org/10.1093/molehr/gav024.

McLennan, I.S., & Pankhurst, M.W., (2015). Anti-müllerian hormone is a gonadal cytokine with two circulating forms and cryptic actions. *Journal of Endocrinology*, 226, R45-57. https://doi.org/10.1530/JOE-15-0206.

Meczekalski, B., Czyzyk, A., Kunicki, M., Podfigurna-Stopa, A., Plociennik, L., Jakiel, G., … Lukaszuk, K. (2016). Fertility in women of late reproductive age: the role of serum anti-Mullerian hormone (AMH) levels in its assessment. *Journal of Endocrinological Investigation*, 39, 1259-1265. https://doi.org/10.1007/s40618-016-0513-x

Merhi, Z. (2019). Vitamin D attenuates the effect of advanced glycation end products on anti-Mullerian hormone signaling. *Molecular and Cellular Endocrinology*, 479, 87-92. https://doi.org/10.1016/j.mce.2018.09.004.

Miyamoto, Y., Skarzynski, D. J., & Okuda, K. (2000). Is tumor necrosis factor alpha a trigger for the initiation of endometrial prostaglandin F(2alpha) release at luteolysis in cattle? *Biology of Reproduction*, 62, 1109-1115. https://doi.org/10.1095/biolreprod62.5.1109.

Mossa, F., & Ireland, J, J. (2019). Physiology and endocrinology symposium: Anti-Mullerian hormone: a biomarker for the ovarian reserve, ovarian function, and fertility in dairy cows. *Journal of Animal Science,* 97, 1446-1455. https://doi.org/10.1093/jas/skz022.

Nahar, A., & Kadokawa, H. (2017). Expression of macrophage migration inhibitory factor (MIF) in bovine oviducts is higher in the postovulatory phase than during the oestrus and luteal phase. *Reproduction, Fertility and Development,* 29, 1521-1529. https://doi.org/10.1071/RD15546.

Osoro, K., & Wright, I. A. (1992). The effect of body condition, live weight, breed, age, calf performance, and calving date on reproductive performance of spring-calving beef cows. *Journal of Animal Science,* 70, 1661-1666. https://doi.org/10.2527/1992.7061661x.

Pfeiffer, K. E., Jury, L. J., & Larson, J. E. (2014). Determination of anti-Müllerian hormone at estrus during a synchronized and a natural bovine estrous cycle. *Domestic Animal Endocrinology*, 46, 58-64. https://doi.org/10.1016/j.domaniend.2013.05.004.

Ribeiro, E. S., Bisinotto, R. S., Lima, F. S., Greco, L. F., Morrison, A., Kumar, A., … Santos, J. E. (2014). Plasma anti-Müllerian hormone in adult dairy cows and associations with fertility. *Journal of Dairy Science,* 97, 6888-6900. https://doi.org/10.3168/jds.2014-7908.

Rodriguez, A., Tripurani, S.K., Burton,J.C., Clementi, C., Larina, I., & Pangas, S.A. (2016). SMAD signaling is required for structural integrity of the female reproductive tract and uterine function during early pregnancy in mice. *Biology of Reproduction,* 95, 1-16. https://doi.org/10.1095/biolreprod.116.139477.

Scheffer, J. A. B., Scheffer, B., Scheffer, R., Florencio, F., Grynberg, M., & Lozano, D. M. (2018). Are age and anti-Müllerian hormone good predictors of ovarian reserve and

response in women undergoing IVF? *JBRA Assisted Reproduction,* 22, 215-220. https://doi.org/10.5935/1518-0557.20180043.

Sefrioui O, Madkour A, Aboulmaouahib S, Kaarouc, I, & Louanjli N. (2019). Women with extreme low AMH values could have in vitro fertilization success. *Gynecological Endocrinology*, 35, 170-173. https://doi.org/10.1080/09513590.2018.1505850.

Skaar, K. S, Nobrega, R. H., Magaraki, A., Olsen, L. C., Schulz, R. W., & Male, R. (2011). Proteolytically activated, recombinant anti Mullerian hormone inhibits androgen secretion, proliferation, and differentiation of spermatogonia in adult zebrafish testis organ cultures. *Endocrinology*, 152, 3527-3540. https://doi.org/10.1210/en.2010-1469.

Tarasconi, B., Tadros, T., Ayoubi, J. M., Belloc, S., de Ziegler, D., & Fanchin, R. (2017). Serum antimullerian hormone levels are independently related to miscarriage rates after in vitro fertilization-embryo transfer. *Fertility and Sterility*, 108, 518-524. https://doi.org/10.1016/j.fertnstert.2017.07.001.

Vandesompele, J., De Preter, K., Pattyn, F., Poppe, B., Van Roy, N., De Paepe, A., & Speleman, F. (2002). Accurate normalisation of real-time quantitative RT-PCR data by geometric averaging of multiple internal control genes. *Genome Biology,* 3, research0034.1–research0034.11. https://doi.org/10.1186/gb-2002-3-7-research0034.

Valdecantos, P.A., Miana, R.D.C.B, García, E.V., García, D.C., Roldán-Olarte, M., & Miceli, D.C. (2017). Expression of bBone morphogenetic protein receptors in bovine oviductal epithelial cells: evidence of autocrine BMP signaling. *Animal Reproduction Science*, 185, 89-96. https://doi.org/10.1016/j.anireprosci.2017.08.006.

Walker, C. G, Meier, S., Mitchell, M. D., Roche, J. R., & Littlejohn, M. (2009). Evaluation

of real-time PCR endogenous control genes for analysis of gene expression in bovine endometrium. *BMC Molecular Biology*, 10, 100. https://doi.org/10.1186/1471-2199-10-100.

Wang, J., Dicken, C., Lustbader, J.W., & Tortoriello, D.V. (2009). Evidence for a Mullerian-inhibiting substance autocrine/paracrine system in adult human endometrium. *Fertility and Sterility*, 91, 1195-1203. https://doi.org/10.1016/j.fertnstert.2008.01.028.

Figure legends

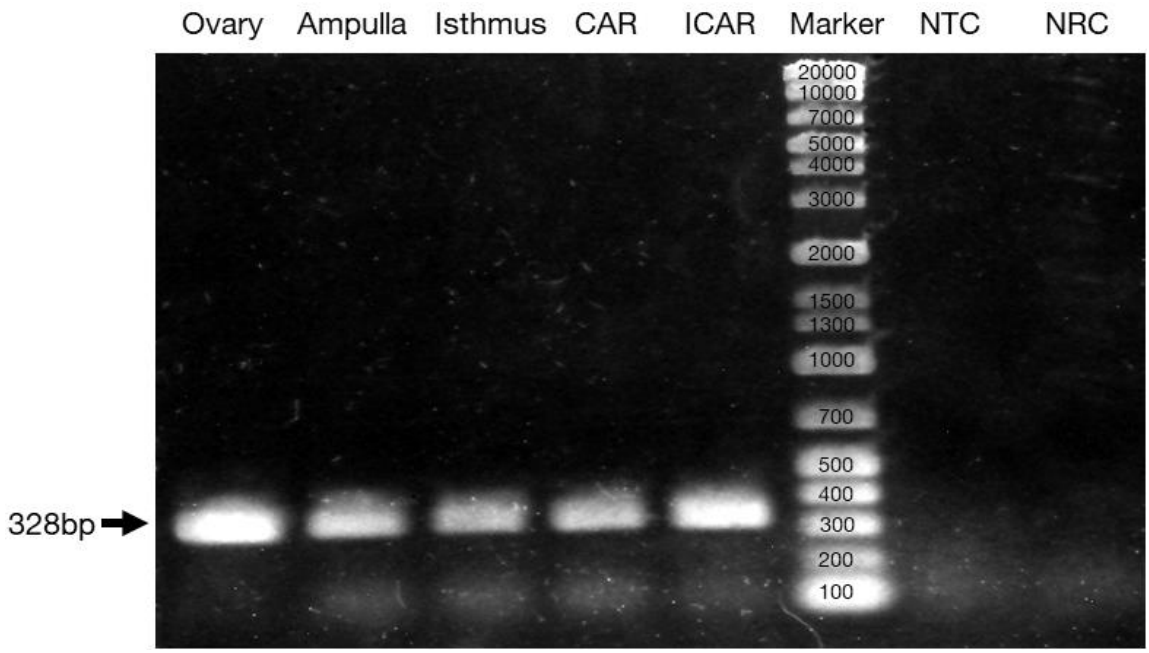

Figure 1. Expression of anti-Müllerian hormone (*AMH*) mRNA, detected by RT-PCR analysis. The electropherogram shows the expected size (328 bp) of PCR products of bovine *AMH* in the ovary, ampulla, isthmus, and caruncular (CAR) and intercaruncular (ICAR) areas of the endometrium in post-pubertal heifers; no amplicons were observed in the no template control (NTC) and no reverse transcription control (NRC) conditions.

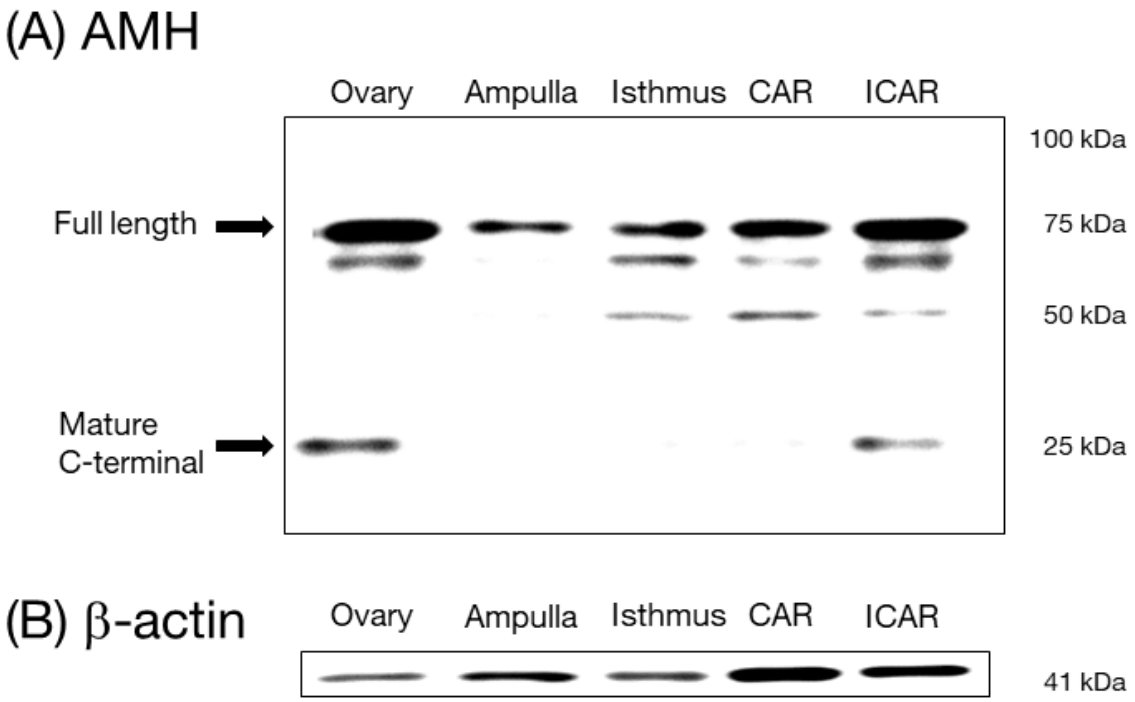

Figure 2. Western blotting using an anti-AMH rabbit antibody on protein extracts of ovaries, ampulla, isthmus, and caruncular (CAR) and intercaruncular (ICAR) areas collected from post-pubertal heifers (a); β–actin was used as a loading control (b).

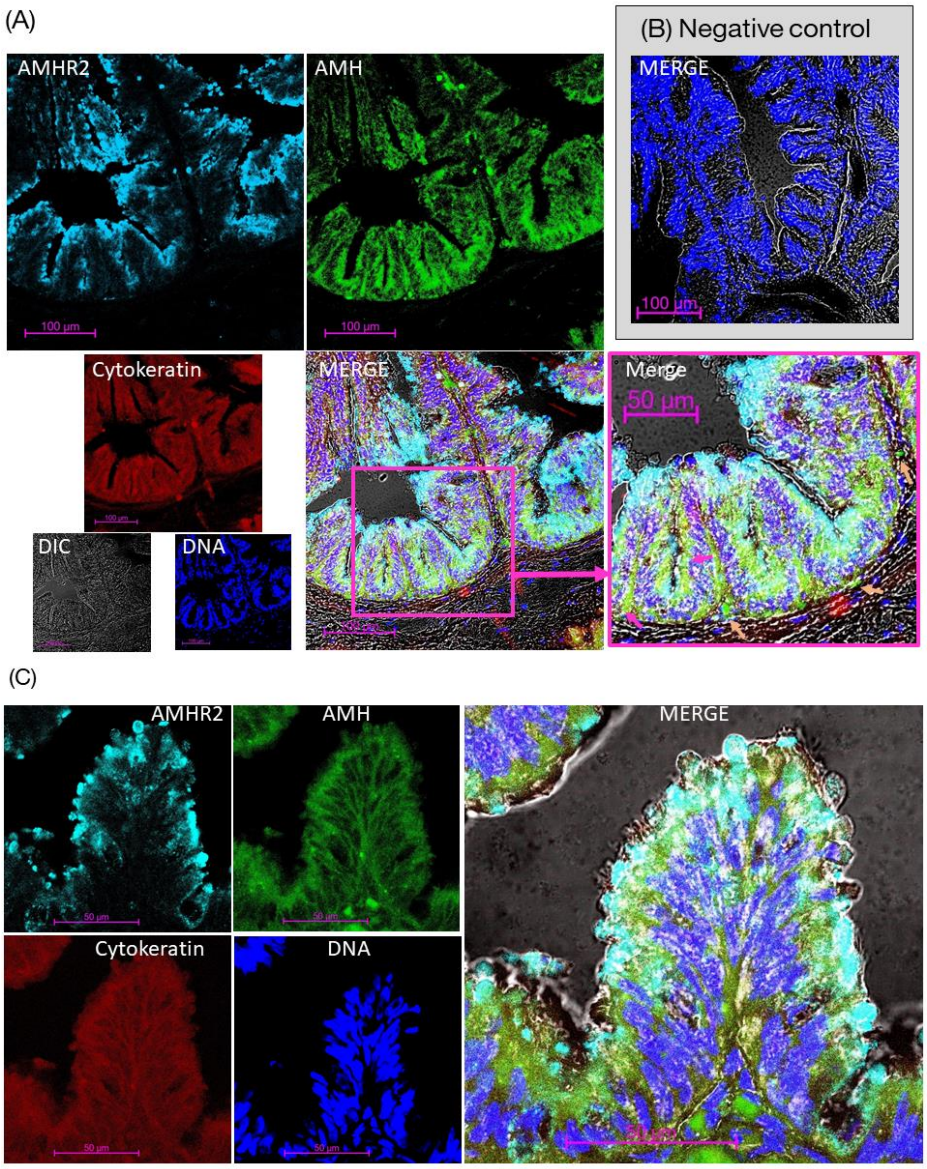

Figure 3. Immunofluorescence staining of AMH in the ampulla samples of post-pubertal heifers. Specimens were collected on day 3 (day 0 = day of estrus). Images were captured via laser-scanning confocal microscopy and show AMHR2 (light blue), AMH (green), cytokeratin (red), and counter-staining with DAPI nuclear stain (dark blue), and differential interference contrast (DIC) microscopy (grayscale). The pink rectangle within the low magnification image indicates the position of the high magnification. In the merged photos,

the pink arrows indicate the AMH signals in the luminal epithelium of mucosa. The brown arrows indicate signals in fibroblasts. Right panel (B) show negative controls staining using the normal animal IgGs. Scale bars represent 100 μm in the low magnification. Scale bars represent 50 μm in the enlarged merge of (A) and (C), and 100 μm in other panels, which shown as pink rectangular.

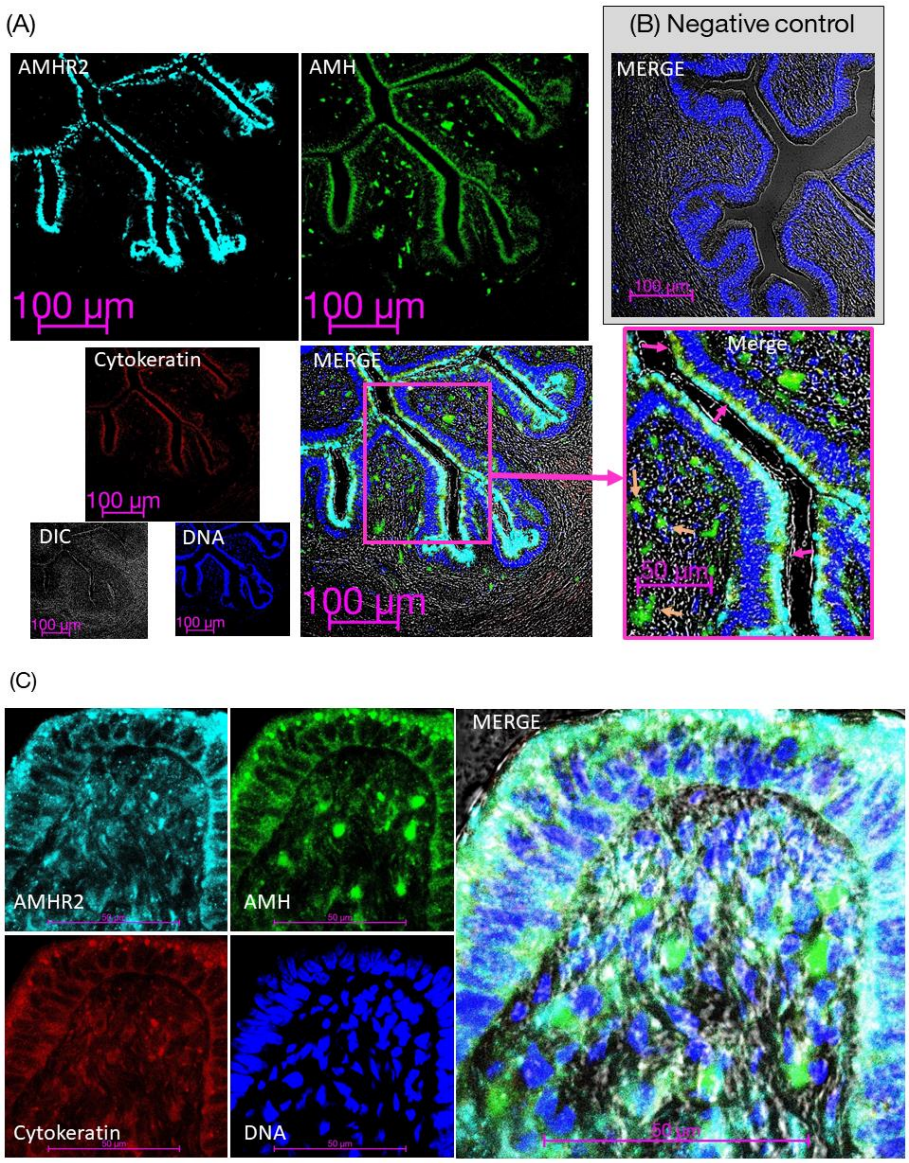

Figure 4. Immunofluorescence staining of AMH in the isthmus samples of post-pubertal heifers. Specimens were collected on day 5 (day 0 = day of estrus). Images were captured via laser-scanning confocal microscopy and show AMHR2 (light blue), AMH (green), cytokeratin (red), and counter-staining with DAPI nuclear stain (dark blue), and differential interference contrast (DIC) microscopy (grayscale). The pink rectangle within the low

magnification image indicates the position of the high magnification. In the merged photos, the pink arrows indicate the AMH signals in the luminal epithelium of mucosa. The brown arrows indicate signals in fibroblasts. Right panel (B) show negative controls staining using the normal animal IgGs. Scale bars represent 100 μm in the low magnification. Scale bars represent 50 μm in the enlarged merge of (A) and (C), and 100 μm in other panels.

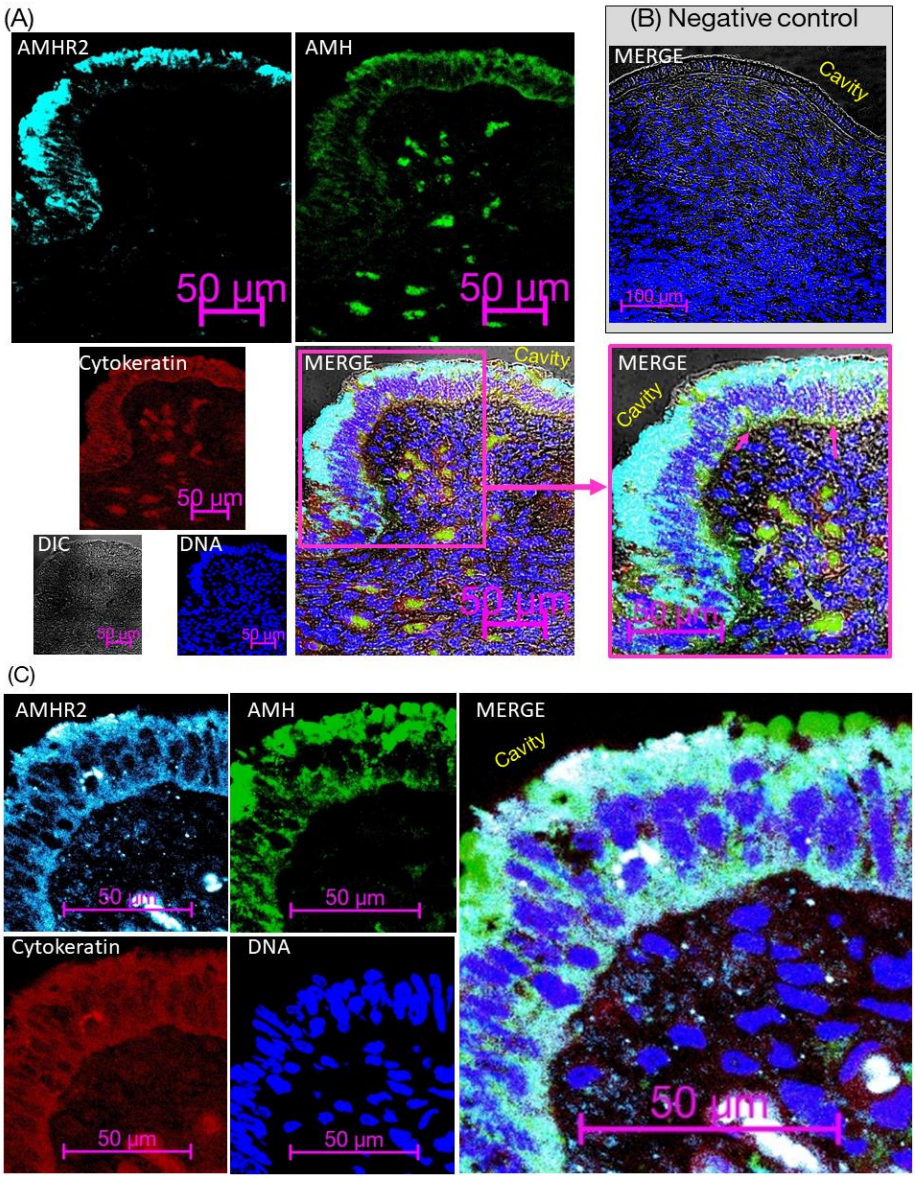

Figure 5. Immunofluorescence staining of AMH in the caruncle samples of post-pubertal heifers. Specimens were collected on day 13. Images were captured via laser-scanning confocal microscopy and show AMHR2 (light blue), AMH (green), cytokeratin (red), and counter-staining with DAPI nuclear stain (dark blue), and DIC microscopy (grayscale). In the merge photos of (A), cavity indicates the uterine cavity. The pink arrows indicate the

AMH signals in the luminal epithelium of caruncle. The green arrows indicate AMH signals in the vasculature. Right panel (B) show negative controls staining using the normal animal IgGs1. Scale bars represent 100 µm in (B), and 50 µm in other panels.

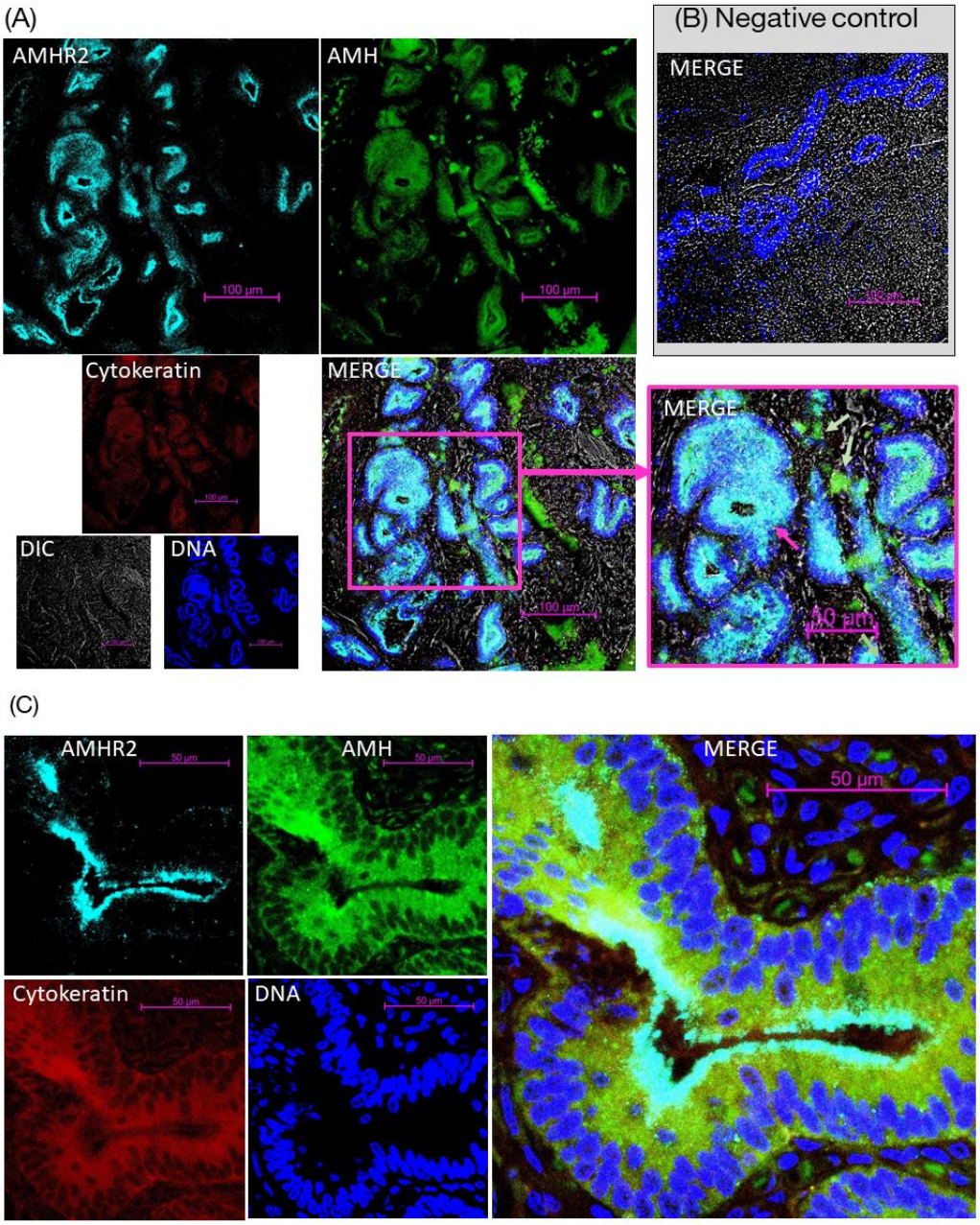

Figure 6. Immunofluorescence staining of AMH in the intercaruncle samples of post-pubertal heifers. Specimens were collected on day 13. Images were captured via laser-scanning confocal microscopy and show AMHR2 (light blue), AMH (green), cytokeratin

(red), and counter-staining with DAPI nuclear stain (dark blue), and DIC microscopy (grayscale). The pink arrows indicate the AMH signals in the epithelium of endometrial glands in intercaruncle. The green arrows indicate AMH signals in the vasculature. Right panel (B) show negative controls staining using the normal animal IgGs. Scale bars represent 50 µm in the enlarged merge of (A) and (C), and 100 µm in other panels.

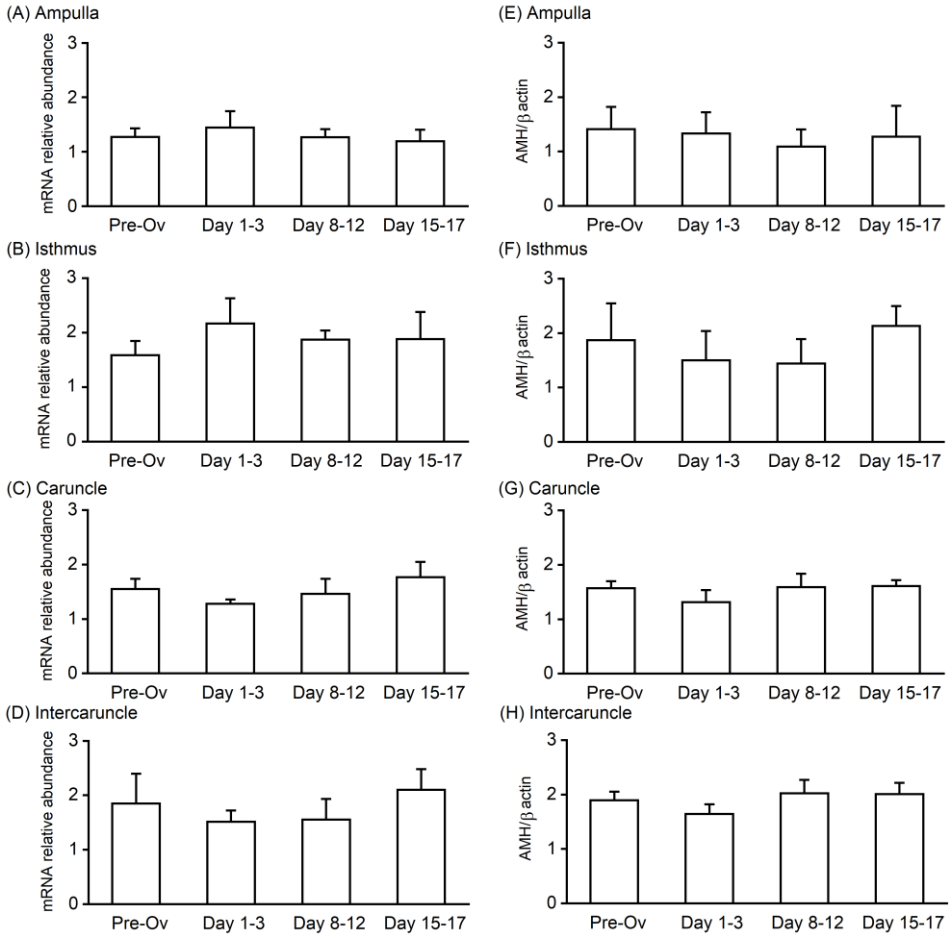

Figure 7. No significant differences in the relative expression levels of *AMH* mRNA (determined by the quantitative RT-PCR) or protein (determined by western blotting) (all data are shown as the mean ± SEM) in the ampulla (A, E), isthmus (B, F), caruncle (C, G), or intercaruncle (D, H) samples of post-pubertal heifers during pre-ovulatory phase (Pre-Ov; day 19 to 21), day 1 to 3, day 8 to 12, or day 15 to 17. Relative *AMH* mRNA levels were determined by quantitative RT-PCR and normalized to the geometric means of *C2orf29* and *SUZ12* levels. Relative AMH protein expression levels were determined by western blotting and normalized to those of β-actin.

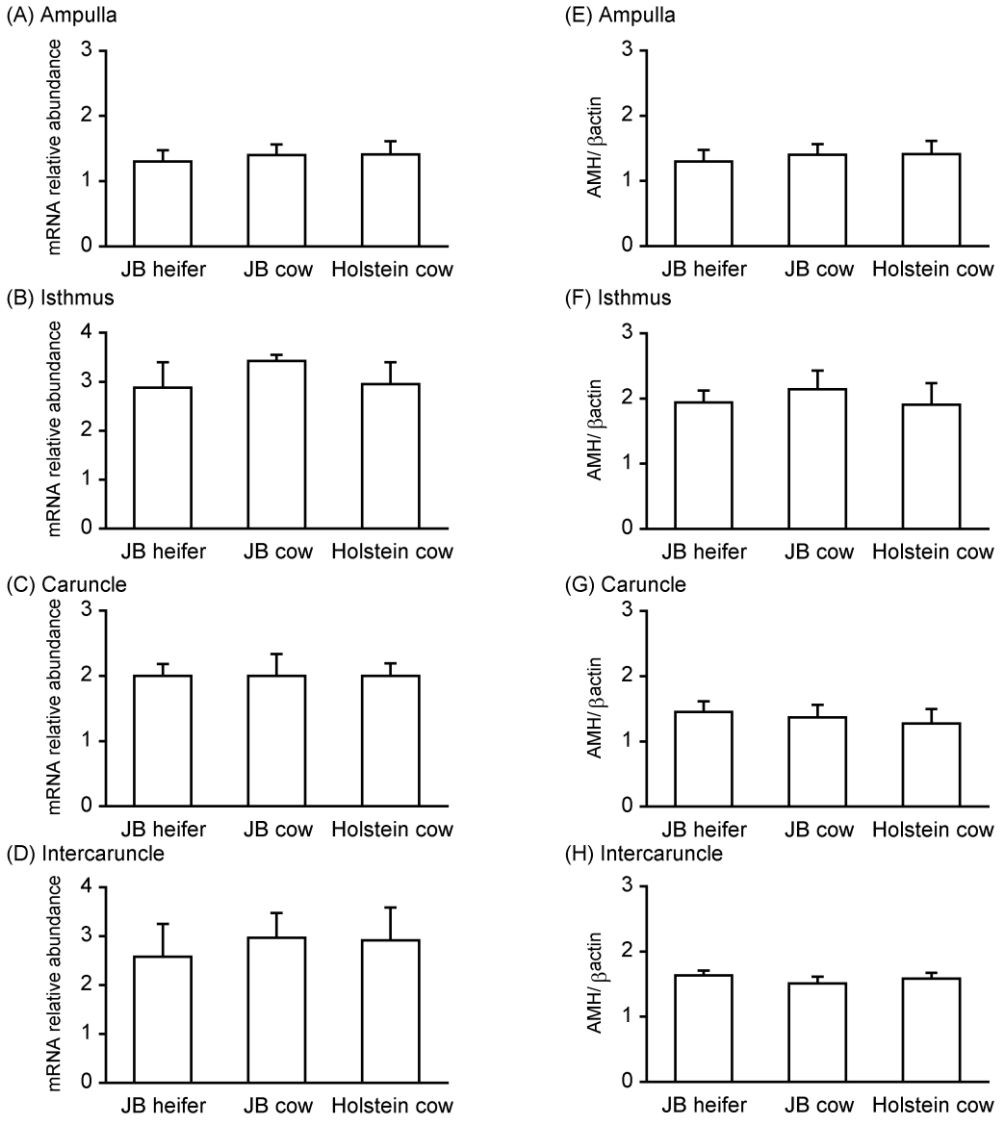

Figure 8. No significant differences in the relative expression levels (shown as the mean ± SEM) of *AMH* mRNA (determined by the quantitative RT-PCR) or protein (determined by western blotting) in the ampulla (A, E), isthmus (B, F), caruncle (C, G), or intercaruncle (D, H) samples among post-pubertal Japanese Black (JB) heifers, JB cows, and Holsteins cows.

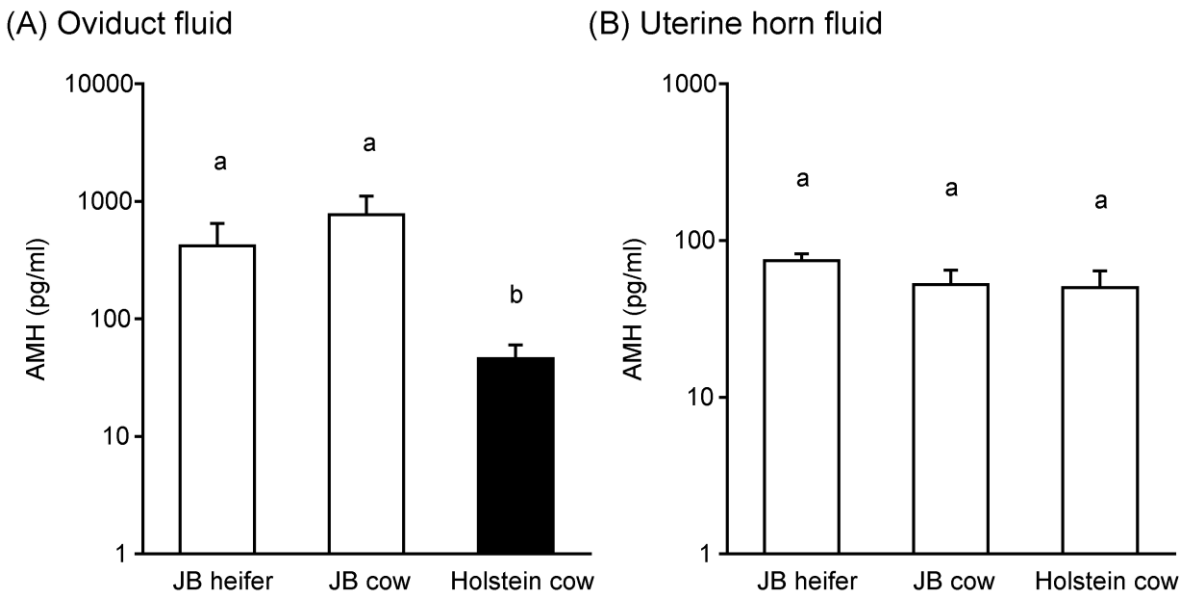

Figure 9. AMH concentrations, as measured by enzyme immunoassays in the oviduct fluid on day 1 to 3 (a) or uterine fluid on day 8 to 14 (b), collected from post-pubertal JB heifers, JB cows, and Holsteins cows. Different letters indicate significant differences ($P < 0.05$) among groups.

Table 1. Details of the primers used for quantitative RT-PCRs

Gene name		Primer sequence 5′-3′	Position		Size (bp)
			Nucleotide	Exon	
AMH	forward	GGGTTAGCCCTTACCCTGC	683–701	3	121
	reverse	GTAACAGGGCTGGGGTCTTT	784–803	4	
C2orf29	forward	TCAGTGGACCAAAGCCACCTA	928–948	3	170
	reverse	CTCCACACCGGTGCTGTTCT	1077–1097	4	
SUZ12	forward	CATCCAAAAGGTGCTAGGATAGAG	1441–1465	13	160
	reverse	TTGGCCTGCACACAAGAATG	1581–1600	14	